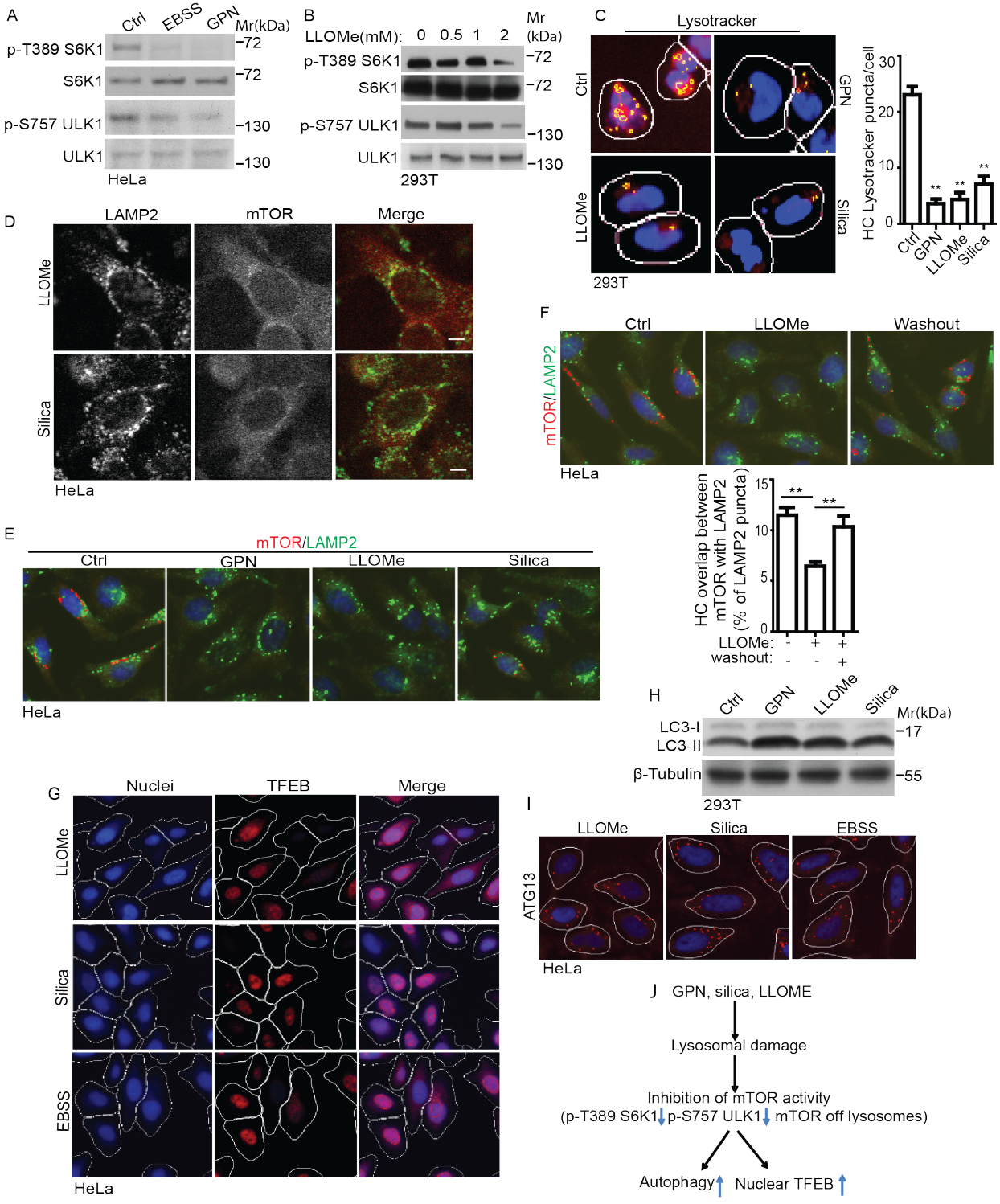

Figure S1, related to Figure 1. Lysosomal damage inhibits mTOR signaling.
(A) Analysis of mTOR activity in HeLa cells treated with 100 μM glycyl-L-phenylalanine 2-naphththylamide (GPN) in full medium or starved in EBSS for 1 h. mTOR activity was monitored by immunoblotting analysis of S6K1 (p-T389) and ULK1 (p-S757) phosphorylation (phosphorylated S6K (T389) and ULK1 (S757) relative to total S6K and

ULK1, respectively). Control (Ctrl), untreated cells. **(B)** Dose-response analysis of mTOR activity in HEK293T cells treated with Leu-Leu-OMe (LLOMe) as indicated in full medium for 1 h. mTOR activity was monitored by immunoblotting as in A. **(C)** HEK293T cells were treated with lysosomal damaging agents (100 μM GPN; 2mM LLOMe; 400 μg/mL Silica) for 1 h in full medium and status of acidified organelles assessed by quantifying LysoTracker Red DND-99 puncta using automated high-content imaging and analysis (HC). None-treated cells were as control (Ctrl). White masks, algorithm defined cell boundaries (primary objects); yellow masks, computer-identified LysoTracker Red puncta (target objects). Data, means ± SEM, n ≥ 3 independent experiments (500 primary objects counted per well; ≥ 5 wells/sample per each experiment), **p < 0.01, ANOVA. **(D)** Immunofluorescence confocal microscopy visualization of mTOR localization relative to LAMP2-positive lysosomes. HeLa cells were treated with 2mM LLOMe or 400 μg/mL Silica in full medium for 1 h, followed by immunostaining of endogenous LAMP2 (green florescence, Alexa-488) and mTOR (red florescence, Alexa-568). Scale bar, 5 μm. **(E)** Sample images from quantification scans using HC analysis of overlaps between mTOR and LAMP2 (corresponding data in Figure 1E) in HeLa cells treated with lysosomal damaging agents for 1 h in full medium. Red and green masks, computer-identified mTOR and LAMP2, respectively (target objects). Control (Ctrl), untreated cells. **(F)** HC analysis of overlaps between mTOR and LAMP2 in HeLa cells treated with 2 mM LLOMe for 1 h followed by 1 h washout (recovery phase) in full medium. Representative images: red and green masks, computer algorithm-identified mTOR and LAMP2 profiles, respectively (target objects). Ctrl, control untreated cells. Data, means ± SEM, n ≥ 3 independent experiments (500 primary objects counted per well; ≥ 5 wells/sample per each experiment), **p < 0.01, ANOVA. **(G)** Representative HC images: TFEB nuclear translocation in HeLa cells treated with 2mM LLOMe or 400 μg/mL Silica in full medium, or starved in EBSS for 1 h. Quantitative data are in Figure 1G. Blue: nuclei, Hoechst 33342; Red: anti-TFEB antibody, Alexa-568. White masks, algorithm-defined cell boundaries (primary objects); pink masks, computer-identified nuclear TFEB based on the average intensity of Alexa-568 fluorescence. **(H)** LC3-II levels in HEK293T cells treated with lysosomal damaging agents (100 μM GPN; 2mM LLOMe; 400 μg/mL Silica) in full medium for 1 h. Ctrl, control untreated cells. **(I)** Examples of HC images: ATG13 puncta in HeLa cells treated as indicated in full medium for 1 h (quantitative HC data, in Figure 1I). White masks, automatically defined cell boundaries (primary objects); red masks, computer-identified ATG13 puncta (target objects). **(J)** Schematic summary of the findings in Figures 1 and S1.

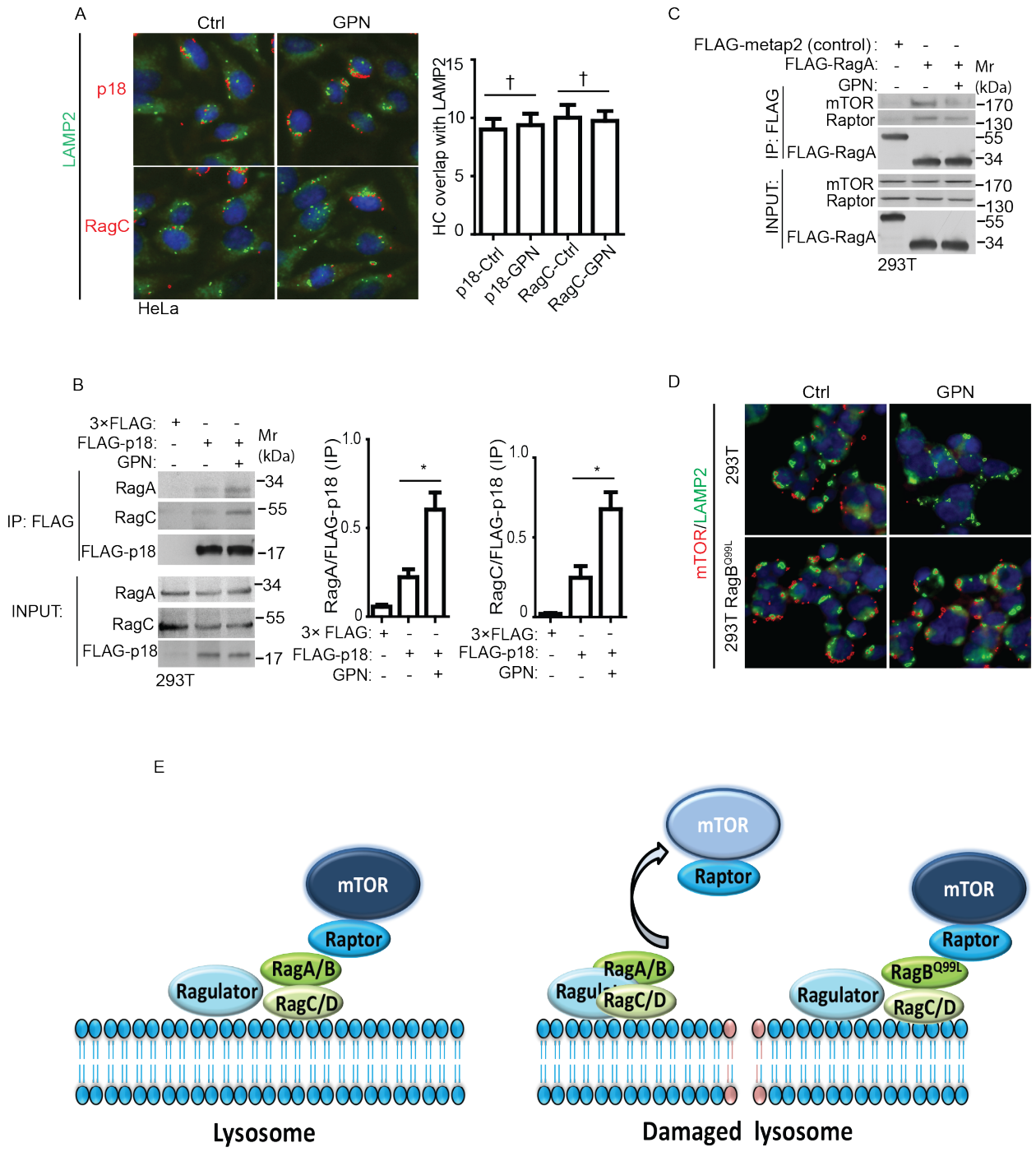

Figure S2, related to Figure 2. Ragulator-Rag complex and mTOR signaling in response to lysosomal damage

(A) HC analysis of overlaps between p18 or RagC and LAMP2 in HeLa cells treated with 100 μM GPN in full medium for 1 h. Representative images shown in left panels. Red and green masks, computer-identified p18 or RagC and LAMP2, respectively (target objects). Ctrl (control): untreated cells. Data, means ± SEM, n ≥ 3 independent experiments (500 primary objects counted per well; ≥ 5 wells/sample per each experiment), † $p \geq 0.05$, ANOVA. **(B)** HEK293T cells expressing FLAG vector or FLAG-

p18 were treated with 100 μM GPN in full medium for 1 h, and cell lysates were subjected to immunoprecipitation with anti-FLAG antibody, followed by immunoblotting analysis of endogenous RagA and RagC. Data, intensity ratio (intensity of RagA or RagC bands normalized to intensity of FLAG-p18 bands in immunoprecipitated material). Data, means ± SEM, n = 3, *p < 0.05, ANOVA. **(C)** Representative images corresponding to quantification by HC in Figure 2F of overlaps between mTOR and LAMP2 in HEK293T cells and HEK293T cells stably expressing constitutively active RagB GTPase ($RagB^{Q99L}$) treated with 100 μM GPN in full medium for 1 h. Red and green masks, computer-identified mTOR and LAMP2, respectively (target objects). **(D)** Immunoprecipitation analysis of interactions between RagA and mTOR/Raptor in cells treated with GPN. HEK293T cells overexpressing FLAG-metap2 (control) or FLAG-RagA were treated with 100 μM GPN in full medium for 1 h. Cell lysates were immunoprecipitated with anti-FLAG antibody and immunoblotted for endogenous mTOR or Raptor. **(E)** Pictorial summary of the results shown in Figures 2 and S2.

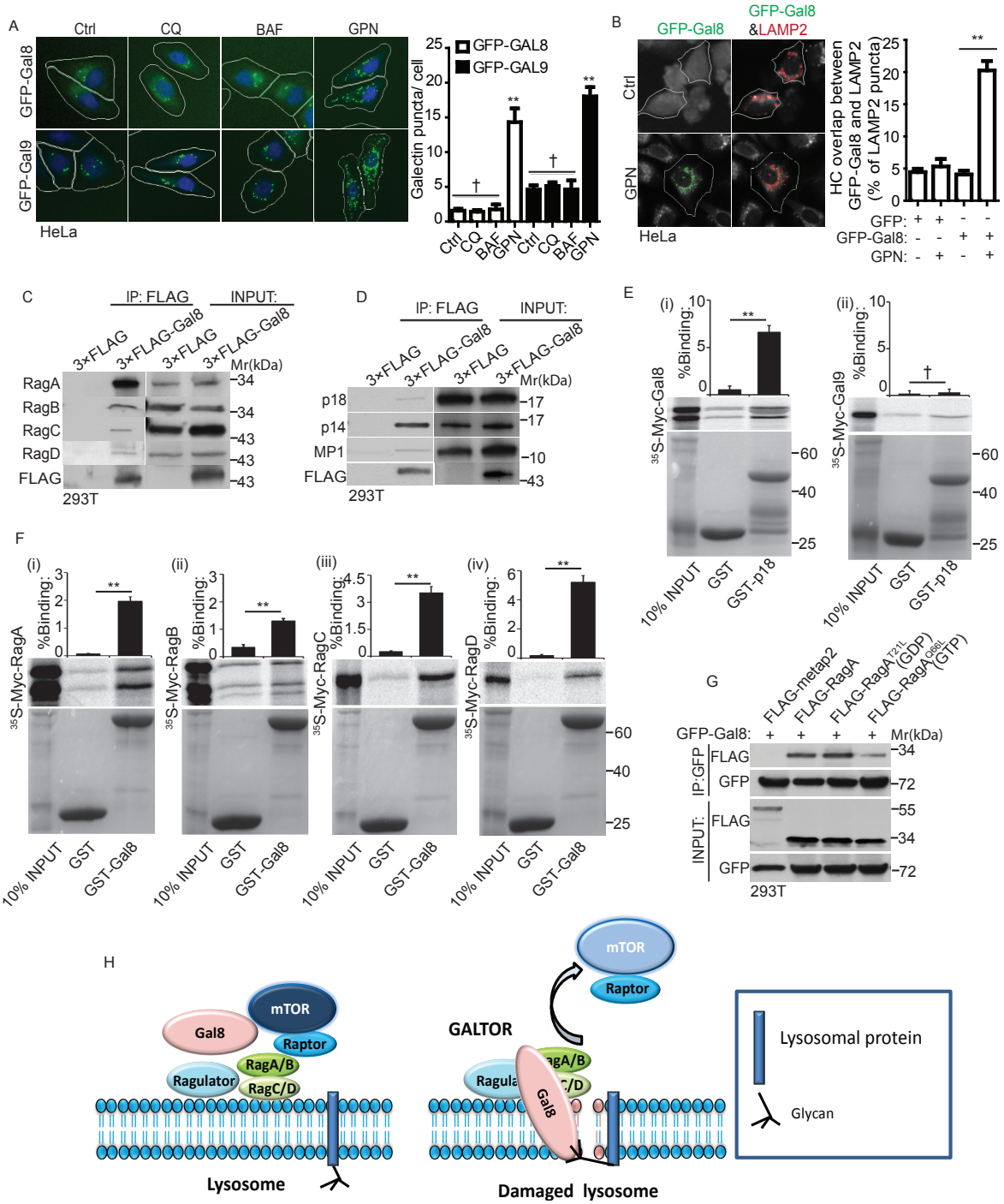

Figure S3, related to Figure 3. Gal8 is in dynamic complexes with the mTOR machinery

(A) HC analysis of the puncta of galectins in response to chloroquine, Bafilomycin A1 and GPN. HeLa cells overexpressing GFP-Gal8 or GFP-Gal9 were treated with 100 μM chloroquine (CQ), 100 μM Bafilomycin A1 (BAF) or 100 μM GPN in full medium for 1 h, and the puncta of GFP-Gal8 or GFP-Gal9 were quantified by HC. White masks, automatically defined cell boundaries (primary objects); green masks, computer-identified GFP-Gal8 or GFP-Gal9 (target objects). Ctrl (control): untreated cells. Data, means ± SEM, n ≥ 3 independent experiments (500 primary objects counted per well; ≥ 5 wells/sample per each experiment), † $p \geq 0.05$, **$p < 0.01$, ANOVA. **(B)** HC analysis of the overlaps between Gal8 and LAMP2 in response to GPN. HeLa cells expressing GFP-Gal8 were treated with 100 μM GPN in full medium for 1 h, and the overlap between GFP-Gal8 and LAMP2 were quantified by HC. White masks, computer algorithm-defined cell boundaries (primary objects); red and green masks, computer-identified LAMP2 and GFP-Gal8 puncta (target objects). Ctrl (control): untreated cells. Data, means ± SEM, n ≥ 3 independent experiments (500 primary objects counted per well; ≥ 5 wells/sample per each experiment), **$p < 0.01$, ANOVA. **(C)** Immunoprecipitation analysis of the interactions between Gal8 and GTPases. HEK293T cells overexpressing FLAG-tagged Gal8 were immunoprecipitated with anti-FLAG beads. Cell lysates and precipitates were blotted for endogenous RagA, B, C, and D. **(D)** Immunoprecipitation analysis of interactions between Gal8 and Ragulator components p14, p18 and MP1. HEK293T cells overexpressing FLAG-tagged Gal8 were immunoprecipitated/collected with anti-FLAG (beads). Cell lysates and collected immune complexes were blotted for endogenous p18, p14, and MP1. **(E)(i-ii)** GST pulldown assay with in vitro translated Myc-tagged Gal8 or Gal9 and GST-tagged p18. GST-tagged p18 immobilized on Gluthatione sepharose beads were incubated with in vitro translated Myc-tagged Gal8 or Gal9 radiolabeled with ^{35}S-methionine. Interactions were assessed by autoradiography. Data (% binding),, means ± SEM, n = 3, † $p \geq 0.05$, **$p < 0.01$, ANOVA. **(F)(i-iv)** GST pulldown assay with in vitro translated Myc-tagged Rag proteins and GST-tagged Gal8. GST-tagged Gal8 immobilized on Gluthatione sepharose beads were incubated with in vitro translated Myc-tagged Rag proteins radiolabeled with ^{35}S-methionine. Interactions were assessed by autoradiography. Data, Data (% binding), means ± SEM, n = 3, **$p < 0.01$, ANOVA. **(G)** Immunoprecipitation analysis of the interactions between Gal8 and RagA GTPase and its mutants. Lysates of HEK293T cells overexpressing GFP-Gal8 and FLAG-tagged metap2 or RagA proteins ($RagA^{WT}$, $RagA^{T21L}$ or $RagA^{Q66L}$) were subjected to anti-GFP immunoprecipitation, followed by immunoblotting for FLAG-tagged RagA proteins. **(H)** Schematic summary of results in Figures 3 and S3, and a model depicting predicted GALTOR complex states based on experimental observations: left, intact lysosome with Gal8 in active (darker shade of blue) mTOR-containing complexes on the cytofacial side of the lysosome limiting membrane; right, upon lysosomal membrane damage, Gal8 gains access to exofacially (lumenally) facing glycoconjugates (represented by a trident), with increased Ragulator-Rags interactions whereas inactive (lighter shade of blue) mTOR-raptor complex dissociates from the lysosome.

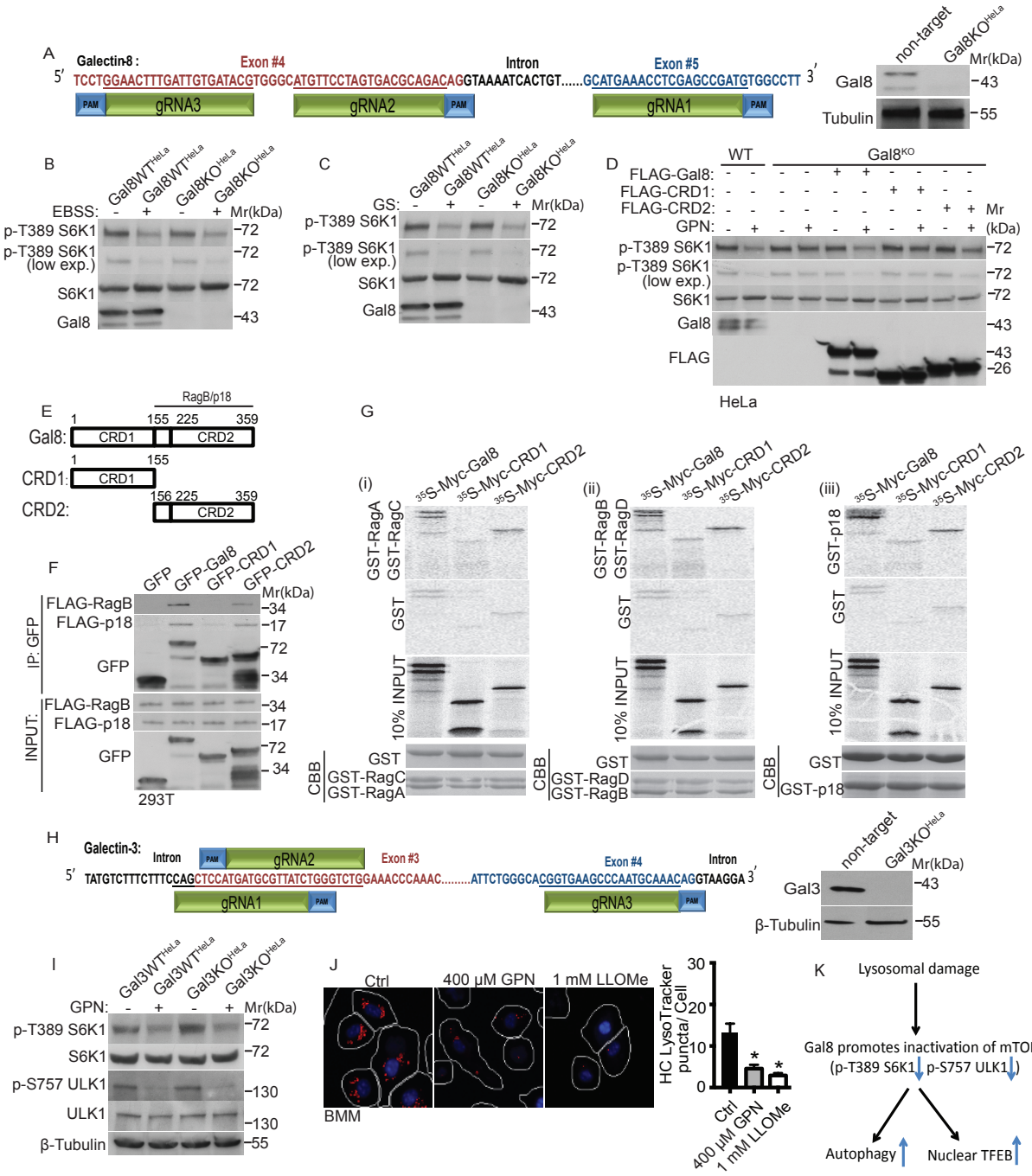

Figure S4, related to Figure 4. Gal8 and Gal3 CRISPR knockouts and response to lysosomal damage.

(A) Schematic for CRISPR/Cas9-mediated knockout strategy of *LGALS8*, and validation of Gal8-knockout (Gal8WT^{HeLa}) by immunoblotting in HeLa cells. **(B)** Immunoprecipitation analysis of mTOR activity in parental HeLa (Gal8WT^{HeLa}) and Gal8-knockout (Gal8KO^{HeLa}) HeLa cells upon EBSS treatment and glucose starvation (GS) **(C)** for 1 h. mTOR activity was monitored by immunoblotting analysis of S6K1

(T389) phosphorylation (phosphorylated S6K (T389) relative to total S6K). **(D)** Immunoprecipitation analysis of mTOR activity in wildtype (WT) and the complementation of Gal8 in Gal8-knockout ($Gal8^{KO}$) HeLa cells upon GPN treatment. $Gal8^{KO}$ HeLa cells overexpressing FLAG-tagged full-length or truncated Gal8 were treated with 100 μM GPN for 1 h in full medium. mTOR activity was monitored by immunoblotting analysis of S6K1 (T389) phosphorylation (phosphorylated S6K (T389) relative to total S6K). **(E)** Schematic diagram of Gal8 domains and deletion constructs. **(F)** HEK293T cells overexpressing GFP-tagged full-length or truncated Gal8 and FLAG-RagB or FLAG-p18 were subjected to anti-GFP immunoprecipitation, followed by immunoblotting for FLAG-RagB or FLAG-p18. **(G)(i)** GST pulldown assay with in vitro translated Myc-tagged Gal8 wildtype or mutants and GST-tagged RagA and RagC. GST-tagged RagA and RagC immobilized on Gluthatione sepharose beads were incubated with in vitro translated Myc-tagged Gal8 wildtype or mutants radiolabeled with ^{35}S-methionine. Interactions were detected by autoradiography. **(ii)** GST pulldown assay with in vitro translated Myc-tagged Gal8 wildtype or mutants and GST-tagged RagB and RagD. GST-tagged RagB and RagD immobilized on Gluthatione sepharose beads were incubated with in vitro translated Myc-tagged Gal8 wildtype or mutants radiolabeled with ^{35}S-methionine. Interactions were detected by autoradiography. **(iii)** GST pulldown assay with in vitro translated Myc-tagged Gal8 wildtype or mutants and GST-tagged LAMTOR1/p18. GST-tagged p18 immobilized on Gluthatione sepharose beads were incubated with in vitro translated Myc-tagged Gal8 wildtype or mutants radiolabeled with ^{35}S-methionine. Interactions were detected by autoradiography. CBB: Coomassie brilliant blue staining. **(H)** Schematic for CRISPR/Cas9-mediated knockout strategy of *LGALS3*, and validation of Gal3-knockout ($Gal3WT^{HeLa}$) by immunoblotting in HeLa cells. **(I)** Analysis of mTOR activity in parental HeLa ($Gal3WT^{HeLa}$) and Gal3-knockout ($Gal3KO^{HeLa}$) HeLa cells treated with 100 μM GPN in full medium for 1 h. mTOR activity was monitored by immunoblotting analysis of S6K1 (T389) and ULK1 (S757) phosphorylation (phosphorylated S6K (T389) and ULK1 (S757) relative to total S6K and ULK1, respectively). **(J)** Primary bone marrow-derived macrophages (BMMs) cells were treated with lysosomal damaging agents for 1 h in full medium and status of acidified organelles assessed by quantifying LysoTracker Red DND-99 puncta using HC. White masks, algorithm-defined cell boundaries (primary objects); red masks, computer-identified LysoTracker Red puncta (target objects). Ctrl (control): untreated cells. Data, means ± SEM, $n \geq 3$ independent experiments (500 primary objects counted per well; ≥ 5 wells/sample per each experiment), $^*p < 0.05$, ANOVA. **(K)** Schematic summary of the results shown in Figures 4 and S4.

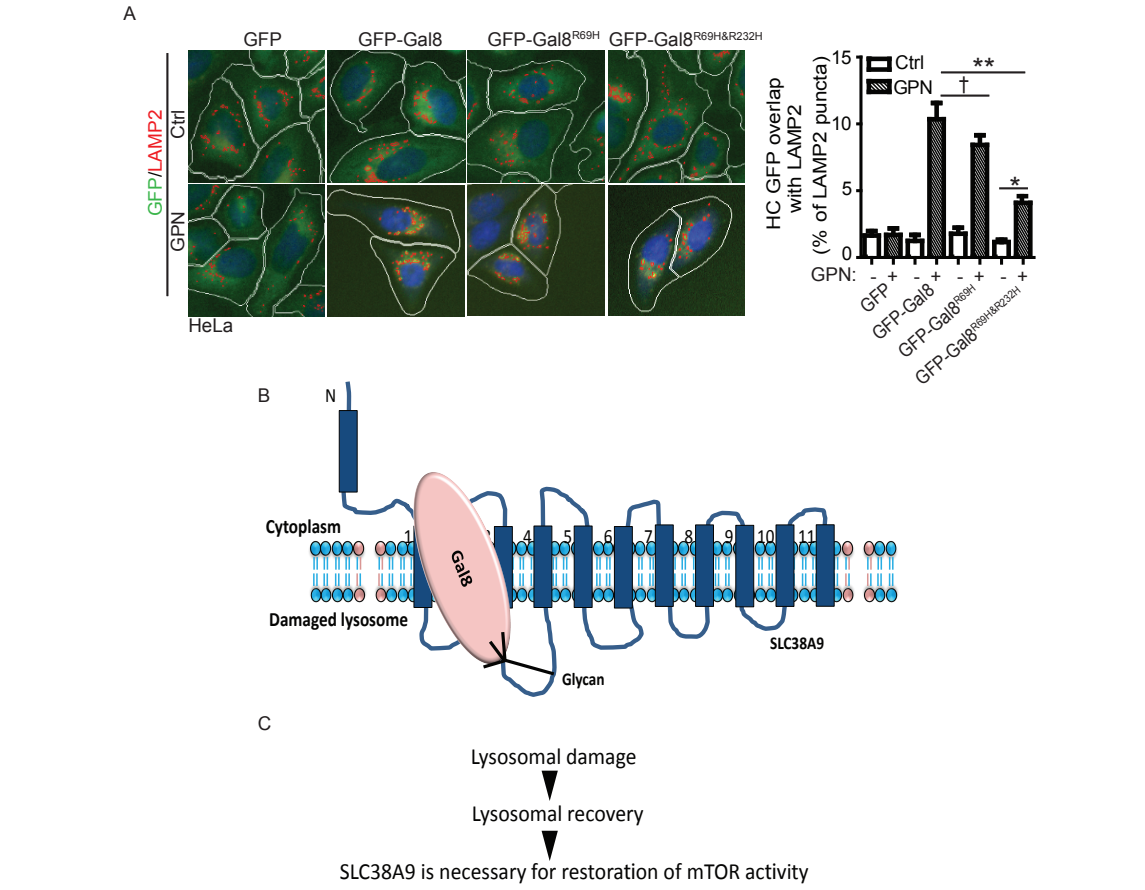

Figure S5, related to Figures 5, 6 and 7. Interactions between Gal8 and SLC38A9 and Gal9 CRISPR knockout effects on AMPK.

(A) Quantification by HC of overlaps between GFP tagged galectin8 (wild type and glycan recognition-mutant forms) and LAMP2 in HeLa cells expressing corresponding plasmids treated with 100 μM GPN for 1 h in full medium. White masks, automatically defined cell boundaries (primary objects); Red and green masks, computer-identified LAMP2 and GFP tagged proteins, respectively (target objects). None-treated cells were as control (Ctrl). Data, means ± SEM, n ≥ 3 independent experiments (500 primary

objects counted per well; ≥ 5 wells/sample per each experiment), † $p \geq 0.05$, *$p < 0.05$, **$p < 0.01$, ANOVA. **(B)** Schematic summary of the results shown in Figure 5. **(C)** Schematic summary of the results shown in Figure 6. **(D)** Schematic diagram for CRISPR/Cas9-mediated knockout of *LGALS9* in HEK293A cells. Gal9-knockout ($Gal9^{KO}$) was validated by Western blotting. **(E)** Analysis of the activation of AMPK in wildtype (WT) and Gal9-knockout ($Gal9^{KO}$) HEK293A cells upon glucose starvation (GS) or 1μM oligomycin treatment **(F)** for 1 h. AMPK activity was monitored by immunoblotting analysis of AMPKα (T172) phosphorylation (phosphorylated AMPKα (T172) relative to total AMPKα).

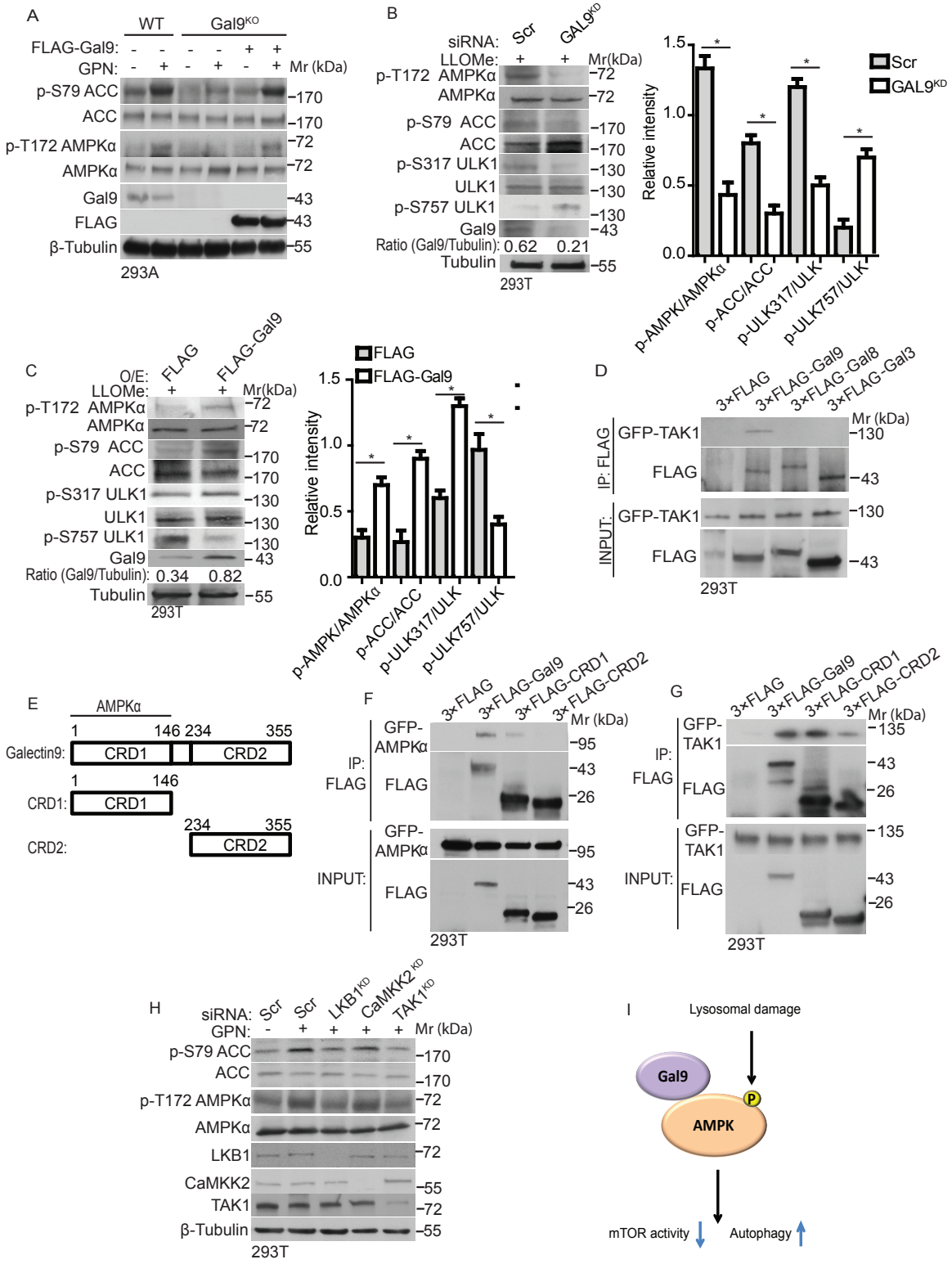

Figure S6, related to Fig. 7. Analysis of Gal9's role in activation of AMPK in response to lysosomal damage

(A) Analysis of the activation of AMPK in wildtype (WT) and the complementation of Gal9 in Gal9-knockout ($Gal9^{KO}$) HEK293A cells treated with 100 μM GPN in full medium for 1 h. AMPK activity was monitored by immunoblotting analysis of AMPKα (T172) and acetyl-CoA carboxylase (ACC, S79) phosphorylation (phosphorylated AMPKα (T172) and ACC (S79) relative to total AMPKα and ACC respectively). **(B)** HEK293T cells transfected with scrambled siRNA (Scr) or Gal9 siRNA ($Gal9^{KD}$) were treated with 2 mM LLOMe in full medium for 1 h, and the cell lysates were analyzed for phosphorylation of indicated proteins. Data, means ± SEM, n = 3, *p < 0.05, ANOVA. **(C)** HEK293T cells overexpressing FLAG-Gal9 were treated with 2 mM LLOMe in full medium for 1 h. Cell lysates were analyzed for the indicated proteins. Data, means ± SEM, n = 3, *p < 0.05, ANOVA. **(D)** Immunoprecipitation analysis of the interactions between galectins and TAK1. HEK293T cells overexpressing FLAG-tagged galectins and GFP-tagged TAK1 were subjected to anti-FLAG immunoprecipitation followed by immunoblotting for GFP-tagged TAK1. **(E)** Schematic diagram of Gal9 domains and deletion constructs**. (F)** HEK293T cells overexpressing FLAG-tagged full-length or truncated Gal9 and GFP-AMPK were subjected to anti-FLAG immunoprecipitation, followed by immunoblotting for GFP-AMPK. **(G)** HEK293T cells overexpressing FLAG-tagged full-length or truncated Gal9 and GFP-TAK1 were subjected to anti-FLAG immunoprecipitation, followed by immunoblotting for GFP-TAK1. **(H)** Analysis of the activation of AMPK in HEK293T cells subjected to knockdowns as indicated treated with 100 μM GPN in full medium for 1 h. AMPK activity was monitored by immunoblotting analysis of AMPKα (T172) and acetyl-CoA carboxylase (ACC, S79) phosphorylation (phosphorylated AMPKα (T172) and ACC (S79) relative to total AMPKα and ACC respectively). Cells transfected with scrambled siRNA were as control (Scr). **(I)** Schematic summary of the results is shown in Figure 7A, B.